

Neutrino Rates in Color Flavor Locked Quark Matter

Sanjay Reddy¹, Mariusz Sadzikowski^{1,2} * and Motoi Tachibana^{1,3} †

¹*Center for Theoretical Physics, Massachusetts Institute of Technology, Cambridge, MA 02139*

²*Institute of Nuclear Physics, Radzikowskiego, 152, 31-342, Kraków, Poland.*

³ *Yukawa Institute for Theoretical Physics, Kyoto University, Kyoto 606-8502, Japan.*

Abstract

We study the weak interaction rates involving Goldstone bosons in the Color Flavor Locked (CFL) quark matter. Neutrino mean free path and the rate of energy loss due to neutrino emission in a thermal plasma of CFL pions and kaons is calculated. We find in addition to neutrino scattering off thermal mesons, novel Cherenkov like processes wherein mesons are either emitted or absorbed contribute to the neutrino opacity. The lack of Lorentz invariance in the medium and the loss of rotational invariance for processes involving mesons moving relative to the medium allow for novel processes such as $\pi^0 \rightarrow \nu\bar{\nu}$ and $e^-\pi^+ \rightarrow \nu_e$. We explore and comment on various astrophysical implications of our finding.

Typeset using REVTeX

*Foundation for Polish Science Fellow

†JSPS Research Fellow

I. INTRODUCTION

QCD at high baryon density is expected to be a color superconductor. For three massless flavors, a symmetric ground state called the Color Flavor Locked (CFL) phase, in which BCS like pairing involves all nine quarks, is favored [1]. This, color superconducting, phase is characterized by a gap in the quark excitation spectrum. Model calculations indicate that the gap $\Delta \sim 100$ MeV for a quark chemical potential $\mu \sim 500$ MeV [2,3]. In this phase the $SU(3)_{\text{color}} \times SU(3)_L \times SU(3)_R \times U(1)_B$ symmetry of QCD is broken down to the global diagonal $SU(3)$ symmetry due to pairing between quarks at the Fermi surface. Gluons become massive by the Higgs mechanism. The lightest excitations in this phase are the nonet of pseudo-Goldstone bosons transforming under the unbroken, global diagonal $SU(3)$ as an octet plus a singlet and a massless mode associated with the breaking of the global $U(1)_B$ symmetry (For a recent review see [4]).

The lack of quark particle-hole excitations in dense quark matter at temperatures less than the critical temperature for color superconductivity ($T_c \sim 0.6\Delta$) will affect the thermodynamic and transport properties of this phase. This can have important astrophysical implications if quark matter were to exist in the core of a neutron star. Several authors have recently explored some aspects of how color superconductivity will impact neutron star observables. These works have provided insight on role of color superconductivity on the phase transition density, the nature of the interface between nuclear matter and CFL matter [5], its response to magnetic fields [6], and the thermal evolution of both young and old neutron stars [7–9]. In this letter we calculate the weak interaction rate for neutrino production and neutrino scattering in the CFL phase and contrast it with earlier estimates of similar rates in normal quark matter.

Neutrinos play a central role in the early and late time thermal evolution of the inner core of the neutron star. Weak interaction rates in the superconducting phase is therefore essential to make connections between color superconductivity and observable aspects associated with neutron star thermal evolution. Neutron stars are born in the aftermath

of a core collapse supernova explosion. The inner core of the newly born neutron star is characterized by a temperature $T \sim 30$ MeV and a lepton fraction (lepton number/baryon number) $Y_L \sim 0.3$ implying $\mu_e \equiv \mu_{\nu_e} - \mu_Q \sim \mu_{\nu_e} \sim 200$ MeV. The high temperature and finite lepton chemical potentials are a consequence of neutrino trapping during gravitational collapse. The ensuing thermal evolution of the newly born neutron star, during which it emits neutrinos copiously, has generated much recent interest [10]. Several aspects of this early evolution can be probed directly since the neutrinos emitted during the first several tens of seconds can be detected in terrestrial detectors such as Super-Kamiokande and SNO. This study is motivated by the prospect that were Color-Flavor-Locked quark matter to exist in the inner core at early times it would result in observable and discernible effects on the supernova neutrino emission.

We can expect significant differences in the weak interaction rates between the normal and the CFL phases since the latter is characterized by a large gap in the quark excitation spectrum. Thus, unlike in the normal phase where quark excitations near the Fermi surface provide the dominant contribution to the weak interaction rates, in the CFL phase, it is the dynamics of the low energy collective states—the flavor pseudo-Goldstone bosons that are relevant. As a first step towards understanding the thermal and transport properties of this phase of relevance to core collapse supernova studies, we identify and calculate the weak interaction rates for neutrino production and scattering. The letter is organized as follows: In §2 we briefly describe the effective theory describing Goldstone bosons in the CFL phase; In §3 we calculate the rate of neutrino reactions of interest; and in §4 we discuss how our findings might affect the early evolution of a newly born neutron star.

II. EFFECTIVE THEORY FOR GOLDSTONE BOSONS

There are several articles that describe in detail the effective theory for the Goldstone bosons in Color-Flavor-Locked quark matter [11–15]. We briefly review some aspects of the effective theory in this section. It is possible to parameterize the effective theory describing

excitations about the $SU(3)$ symmetric CFL ground state in terms of the two fields $B = e^{i\beta/f_B}$ and $\Sigma = e^{2i(\pi/f_\pi + \eta'/f_A)}$, representing the Goldstone bosons of broken baryon number β , and of broken chiral symmetry, the pseudo-scalar octet π , and the pseudo-Goldstone boson η' , arising from broken approximate $U(1)_A$ symmetry. Since our primary interest here is to calculate the charged and neutral current weak interactions we will ignore the β and η' fields and retain only the π fields describing pions and kaons in the CFL phase. Turning on nonzero quark masses, explicitly breaks chiral symmetry and induces a gap in the spectrum as the Goldstone bosons acquire a mass due to this explicit breaking of chiral symmetry. In addition, dissimilar quark masses induce new stresses on the system, acting in a manner analogous to an applied flavor chemical potential and favoring meson condensation. This was recently pointed out by Bedaque and Schafer [16]. In this work we include the stress induced by the strange quark mass, but we will assume that it is not strong enough to result in the meson condensation ¹.

The leading terms in the effective Lagrangian describing the octet Goldstone boson field π is given by

$$\begin{aligned}\mathcal{L} = & \frac{1}{4}f_\pi^2 \left[\text{Tr} \nabla_0 \Sigma \nabla_0 \Sigma^\dagger - v^2 \text{Tr} \vec{\nabla} \Sigma \cdot \vec{\nabla} \Sigma^\dagger \right] \\ & + f_\pi^2 \left[\frac{a}{2} \text{Tr} \tilde{M} (\Sigma + \Sigma^\dagger) + \frac{\chi}{2} \text{Tr} M (\Sigma + \Sigma^\dagger) \right] \\ & \nabla_0 \Sigma = \partial_0 \Sigma - i [X_L \Sigma - \Sigma X_R] .\end{aligned}\tag{1}$$

The decay constant f_π has been computed previously [12] and is proportional to the quark chemical potential. $X_{L,R}$ are the Bedaque-Schafer terms: $X_L = -\frac{MM^\dagger}{2\mu}$, $X_R = -\frac{M^\dagger M}{2\mu}$, and $\tilde{M} = |M|M^{-1}$. At asymptotic densities, where the instanton induced interactions are highly suppressed and the $U(1)_A$ symmetry is restored, the leading contributions to meson masses arise from the $\text{Tr} \tilde{M} \Sigma$ operator whose coefficient a has been computed and is given

¹If K^0 condensation occurs, as discussed in Ref. [16,17] the ground state is reorganized and the excitation spectrum is modified. The weak interaction rates in this phase is currently under investigation and will be reported elsewhere.

by $a = 3 \frac{\Delta^2}{\pi^2 f_\pi^2}$ [12,15]. At densities of relevance to neutron stars the instanton interaction may become relevant. In this case a $\langle \bar{q}q \rangle$ condensate is induced [13,18] and consequently the meson mass term can receive a contribution from the operator $\text{Tr} M \Sigma$. Its coefficient χ at low density is sensitive to the instanton size distribution and form factors. Current estimates indicate that the instanton contribution to K^0 mass can lie in the range 5 – 120 MeV [18]. In this article we will assume that the instanton contribution to the K^0 mass is ~ 50 MeV ($\chi \sim 15$ MeV) at $\mu = 400$ MeV and $\Delta = 100$ MeV. With this choice, the kaon mass is too large to allow for K^0 condensation. The meson masses are explicitly given by

$$\begin{aligned} m_{\pi^\pm}^2 &= a(m_u + m_d)m_s + \chi(m_u + m_d) \\ m_{K^\pm}^2 &= a(m_u + m_s)m_d + \chi(m_u + m_s) \\ m_{K^0}^2 &= a(m_d + m_s)m_u + \chi(m_d + m_s). \end{aligned} \quad (2)$$

To incorporate weak interactions, we gauge the Chiral Lagrangian in the usual way by replacing the covariant derivative by [19]

$$\begin{aligned} D_\mu \Sigma &= \nabla_\mu \Sigma - \frac{ig}{\sqrt{2}}(W_\mu^+ \tau^+ + W_\mu^- \tau^-) \Sigma \\ &\quad - \frac{ig}{\cos \theta_W} Z_\mu (\tau_3 \Sigma - \sin \theta_W^2 [Q, \Sigma]) - i \tilde{e} \tilde{A} [Q, \Sigma] \end{aligned} \quad (3)$$

The time component of ∇_μ includes the Bedaque-Schafer term as described above. The fields W_μ^\pm, Z_μ describe weak gauge bosons. The charge matrix is diagonal $Q = \text{diag}(\frac{2}{3}, -\frac{1}{3}, -\frac{1}{3})$ as well as weak-isospin matrix $\tau_3 = \frac{1}{2} \text{diag}(1, -1, -1)$ whereas τ^+ and τ^- are the isospin raising and lowering operators which incorporate Cabbibo mixing. The weak coupling constant is related to Fermi coupling constant via the standard relation $\sqrt{2}g^2 = 8G_F M_W^2$ where M_W is a mass of the W gauge boson and the mass of Z boson $M_Z \cos \theta_W = M_W$ where θ_W is Weinberg angle. The last term is the modified electromagnetic coupling of mesons to the massless \tilde{A} photon in the CFL phase, where the charge $\tilde{e} = e \cos \theta$ and θ is the mixing angle between the original photon and the eighth gluon [6].

For momenta small compared to f_π we can expand the nonlinear chiral Lagrangian to classify diagrams as the first order (proportional to f_π) and the second order (independent

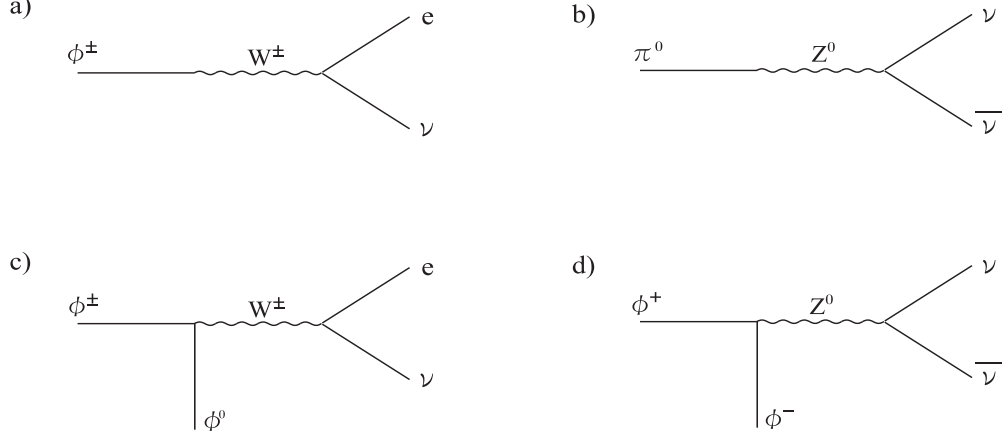


FIG. 1. Feynman graphs showing the coupling of the neutral and charged leptonic current to one and two meson states.

of f_π). The first order diagrams, involving two leptons and a meson are shown in the Fig. 1. In Fig. 1(a) the charged current decay of charged pions and kaons is shown. Fig. 1(b) shows the neutral current decay of $\pi^0 \rightarrow \nu\bar{\nu}$. In vacuum, the latter process is forbidden by angular momentum conservation. However, as we will show later, it is allowed for finite momentum pions in the CFL medium. Diagrams in the Fig. 1(c) and 1(d) show processes involving two mesons. The process in Fig. 1(c) is the two body correction to the charged current decay of the decay of charged kaons and pions interacting with the neutral mesons. And Fig. 1(d) depicts neutrino pair emission from the annihilation of charged Goldstone bosons K^\pm and π^\pm and neutrino-meson scattering.

The amplitudes for the leading order processes are given by

$$A_{\pi^0 \rightarrow \nu\bar{\nu}} = G_F f_\pi \tilde{p}_\mu j_Z^\mu \quad (4)$$

$$A_{\pi^\pm \rightarrow e\nu} = G_F f_\pi \cos\theta_C \tilde{p}_\mu j_W^\mu$$

$$A_{K^\pm \rightarrow e\nu} = G_F f_\pi \sin\theta_C p_\mu j_W^\mu$$

where $\tilde{p}_\mu = (E, v\vec{p})$ is the modified four-momentum of Goldstone boson and j_W^μ and j_Z^μ describe the charged leptonic current and neutral leptonic currents. θ_C is the Cabbibo mixing angle. Note that the meson "four momenta" that appear in the matrix element do not correspond to the on shell four momenta of the mesons. This is because the covariant

derivatives contains the in medium velocity and for the case of kaons, the energy shift arising from the Bedaque-Schafer term.

At next to leading order, the amplitude is independent of f_π . The amplitude for the charged current process is given by

$$A_{\Phi^\pm \Phi^0 \rightarrow e\nu} = -iC \frac{G_F}{2} (\tilde{p}_1 - \tilde{p}_2)_\mu j_W^\mu \quad (5)$$

where the coupling coefficient $C = \sin \theta_C$ for $\pi^0 K^-, \pi^0 K^+$; $C = \sqrt{2} \sin \theta_C$ for $\pi^- \bar{K}^0, \pi^+ K^0$; $C = \sqrt{2} \cos \theta_C$ for $K^- K^0, K^+ \bar{K}^0$ and $C = 2 \cos \theta_C$ for $\pi^- \pi^0, \pi^+ \pi^0$. Neutrinos couple to the charged mesons via the neutral current. This leads to process such as the annihilation of $\pi^+ \pi^- \rightarrow \nu \bar{\nu}$ and $K^+ K^- \rightarrow \nu \bar{\nu}$, whose amplitude is given by

$$A_{\Phi^+ \Phi^- \rightarrow \nu \bar{\nu}} = -i \frac{G_F}{\sqrt{2}} (1 - 2 \sin^2 \theta_W) (\tilde{p}_1 - \tilde{p}_2)_\mu j_Z^\mu \quad (6)$$

where p_1, p_2 are momenta of Goldstone bosons. It also gives rise to neutral current neutrino-meson scattering given by the amplitude

$$A_{\nu \Phi^\pm \rightarrow \nu \Phi^\pm} = -i \frac{G_F}{\sqrt{2}} (1 - 2 \sin^2 \theta_W) (\tilde{p}_1 + \tilde{p}_2)_\mu j_Z^\mu. \quad (7)$$

III. THERMODYNAMICS AND NEUTRINO RATES

The dispersion relations for the Goldstone modes in the CFL phase are unusual. They are easily computed by expanding the Lagrangian to second order in the meson fields and are given by

$$\begin{aligned} E_{K^\pm} &= \mp \frac{m_s^2}{2\mu} + \sqrt{v^2 p^2 + m_{K^\pm}^2} & E_{\pi^\pm} &= \sqrt{v^2 p^2 + m_{\pi^\pm}^2} \\ E_{K^0} &= -\frac{m_s^2}{2\mu} + \sqrt{v^2 p^2 + m_{K^0}^2} & E_{\bar{K}^0} &= \frac{m_s^2}{2\mu} + \sqrt{v^2 p^2 + m_{K^0}^2} \end{aligned} \quad (8)$$

They violate Lorentz invariance and the induced effective chemical potential arising from the analysis of Bedaque and Schafer [16] breaks the energy degeneracy of the positive and negative charged kaons making the K^+ lighter than the K^- . The latter effect, naturally

results in an excess positive charge in the meson sector at finite temperature. Electric charge neutrality of this phase demands electrons and consequently an electric charge chemical potential is induced. This novel phenomena, akin to the thermoelectric effect, modifies the number densities of the individual mesons in the plasma.

The number densities of the kaons, pions and the total electric charge density of the meson gas, normalized to the photon number are shown in Fig. 2. The results are shown as a function of temperature for a quark chemical potential of 400 MeV (corresponding to $f_\pi = 83$ MeV) at which we have chosen the pairing gap $\Delta = 100$ MeV. The quark masses are set at $m_u = 3.75$ MeV $m_d = 7.5$ MeV and $m_s = 150$ MeV and instanton induced coefficient of the $\text{Tr}M\Sigma$ operator $\chi = 16$ MeV as mentioned earlier. With these assumptions, at zero temperature the rest energies of mesons are given by: $E_{\pi^\pm} \simeq 30$ MeV; $E_{K^+} \simeq 26$ MeV; $E_{K^-} \simeq 82$ MeV ; $E_{K^0} \simeq 24$ MeV and $E_{\bar{K}^0} \simeq 80$ MeV. It is at first surprising that the plasma has more mesons than photons. Despite being massive, the meson number is enhanced for two reasons. First, the velocity factor $v = 1/\sqrt{3}$ results in a soft dispersion relation resulting in reduced Boltzmann suppression of the high momentum modes. It is easily seen that number density is enhanced by the factor $1/v^3$. Secondly, the presence of the Bedaque and Schafer term which acts like an effective chemical potential for anti-strangeness and the induced negative electric charge chemical potential required to maintain charge neutrality enhances the number of mesons carrying anti-strangeness and negative charge at low temperature.

Prior to discussing the neutrino rates in the finite temperature plasma we briefly comment on the temperature range over which our analysis is expected to be valid. The effective theory description of the finite temperature phase is valid only if the typical meson energy is small compared to 2Δ . For larger energies, meson propagation is strongly attenuated since they can decay into quark quasi-particle excitations. Further, with increasing temperature, we should expect the coefficients of the effective theory such as f_π, v and the meson masses change. On general grounds we expect these changes to become relevant as T approaches T_c . In our analysis we ignore these changes and restrict ourselves to temperatures T small

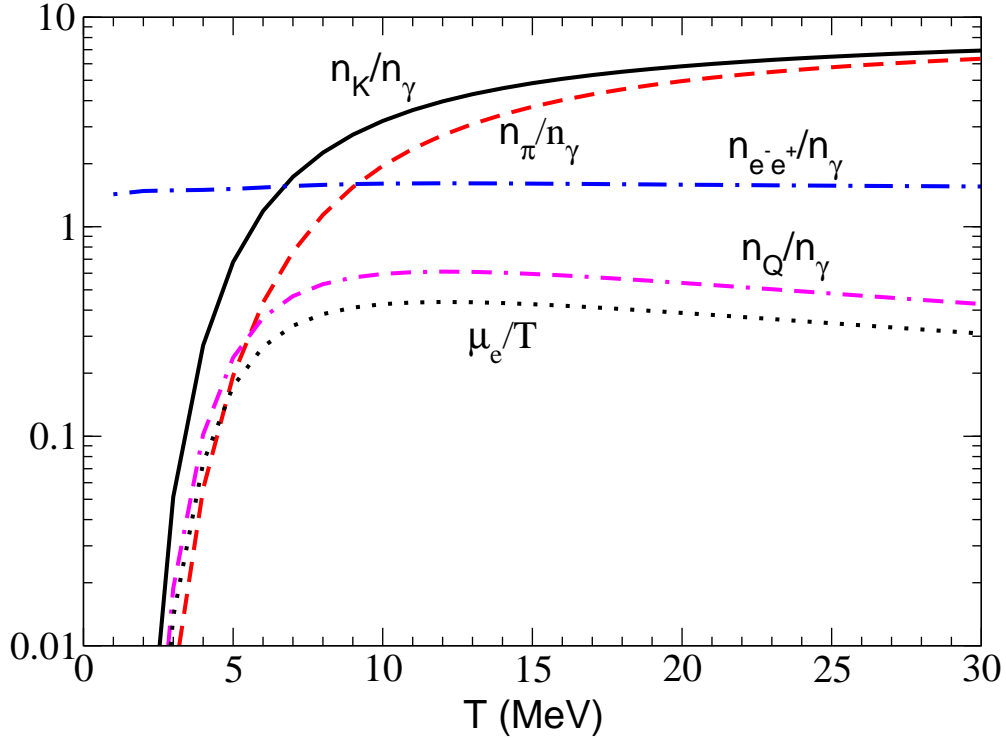


FIG. 2. Number densities of the mesons, the charge density and the number of e^+e^- pairs, normalized by the photon number density. The electron chemical potential required to maintain electric charge neutrality at finite temperature is also shown.

compared to T_c . At $\mu = 400$ MeV and $\Delta = 100$ MeV corresponding to $T_c \sim 60$ MeV we expect our analysis to provide a fair description of the plasma for $T \lesssim 30$ MeV ².

A. Neutrino Opacity

Novel processes such as the $\nu \rightarrow \pi^0 \nu$ and $\nu_e \rightarrow \pi^+ e^-$ are allowed in this phase owing to the fact that mesons can have a space like dispersion relation. These processes can be thought of as arising due to Cherenkov radiation of mesons. The dispersion relation for the pions and kaons indicate that they possess space like four momenta when their 3-momentum

²Assuming that temperature dependence of $\Delta(T) = \Delta_0 \sqrt{1 - (T/T_c)^2}$ at $T = 30$ MeV the gap is reduced by only 15 percent.

satisfy:

$$p_\pi > \frac{m_\pi}{\sqrt{1-v^2}} \quad ; \quad p_K > \frac{\sqrt{m_K^2(1-v^2) + X^2} - X}{1-v^2}, \quad (9)$$

where $X = m_s^2/(2\mu)$ for anti-kaons and $X = -m_s^2/(2\mu)$ for kaons.

We can define the neutrino mean free path for these processes as the neutrino velocity times the rate of emission of Cherenkov mesons. This is given by

$$\frac{1}{\lambda_{\nu \rightarrow \phi l}(E_\nu)} = \frac{1}{2E_\nu} \int \frac{d^3 p_\phi}{(2\pi)^3 2E_\phi} \int \frac{d^3 p_l}{(2\pi)^3 2E_l} (2\pi)^4 \delta^4(P_\nu - P_\phi - P_l) |A_{\nu \rightarrow \phi l}|^2 \quad (10)$$

where E_ν is the initial neutrino energy, p_ϕ is the meson momentum and p_l is the final state lepton momentum. We label the final state lepton as l to account for the fact that it could be either a neutrino or an electron. The amplitude for this process was calculated earlier and is proportional to f_π . Since these processes do not have any mesons in the initial state they can occur at zero temperature and in our analysis the rate for the process depends on the neutrino energy and is independent of the temperature in so far as the meson masses and f_π is independent of temperature. These processes occur only when the neutrino energy is above the threshold given by $E_{th} = m/\sqrt{1-v^2}$, where m is mass of the emitted meson and v its velocity.

Low energy neutrinos can absorb a thermal meson and scatter into either a final state neutrino by the process $\nu + \pi^0 \rightarrow \nu$, or into a final state electron by the process $\nu_e + \pi^- \rightarrow e^-$. These processes are temperature dependent as they are proportional to the density of mesons in the initial state. As before, since the process involves only one meson the matrix element is of order f_π . The mean free path due to these processes is easily computed using the relation

$$\frac{1}{\lambda_{\nu \phi \rightarrow l}(E_\nu)} = \frac{1}{2E_\nu} \int \frac{d^3 p_\phi}{(2\pi)^3 2E_\phi} f(E_\phi) \int \frac{d^3 p_l}{(2\pi)^3 2E_l} (2\pi)^4 \delta^4(P_\nu + P_\phi - P_l) |A_{\nu \phi \rightarrow l}|^2 \quad (11)$$

where $f(E_\phi)$ is the Bose distribution function for the initial state mesons.

In contrast to processes involving the emission or absorption on mesons by neutrinos, the usual scattering process involves the coupling of the neutrino current to two mesons. As

noted earlier, the amplitude for these processes is suppressed by the factor p/f_π where p is the meson momentum. However, in this case the kinematics is not restricted to involve only space like mesons. The neutrino mean free path for the scattering process is given by

$$\frac{1}{\lambda_{\nu\phi^\pm \rightarrow \nu\phi^\pm}(E_\nu)} = \frac{1}{2E_\nu} \int \frac{d^3p_\phi}{(2\pi)^3 2E_\phi} f(E_\phi) \int \frac{d^3p'_\nu}{(2\pi)^3 2E'_\nu} \int \frac{d^3p'_\phi}{(2\pi)^3 2E'_\phi} \times (2\pi)^4 \delta^4(P_\nu + P_\phi - P'_\phi - P_\nu) |A_{\nu\phi^\pm \rightarrow \nu\phi^\pm}|^2 \quad (12)$$

The resulting neutrino mean free path for all three classes of processes discussed above is shown in Fig. 3. The results are presented as a function of the ambient temperature. We assume that the typical neutrino energy is determined by the local temperature and set $E_\nu = \pi T$ since this corresponds to mean energy of neutrinos in thermal equilibrium. Note that for the Cherenkov process there is no intrinsic temperature dependence and the temperature dependence of the results shown arise because we have set $E_\nu = \pi T$. At low temperature, or equivalently, for neutrino energy small compared to the pion mass the Cherenkov process is kinematically forbidden and dominant source of opacity are those involving mesons in the initial state. The resulting mean free path for each of these processes is shown in the figure. Charged current reactions involving the absorption or emission of kaons are Cabbibo suppressed and contribute to less than a few percent of the total rate at high temperature (At lower temperature, despite the Cabbibo suppression, reactions involving the K^+ can become important as they are the most abundant charged mesons in the plasma). At high temperature the meson number density dominates over the electron-positron number density and we are justified in neglecting the contribution of neutrino-electron and neutrino-positron scattering to the opacity. At low temperature ($T \lesssim 5$ MeV), these processes can also be an additional source of opacity. We have not included this in our study here since at these low temperatures the mean free path are typically larger than the neutron star radius. The total contribution to opacity of novel processes involving only one meson is also shown in the figure as a solid curve labelled ν_{3B} . As expected, at low temperature these processes dominate over the usual neutrino-meson neutral current scattering since their amplitude is proportional to f_π . The total neutrino opacity due to

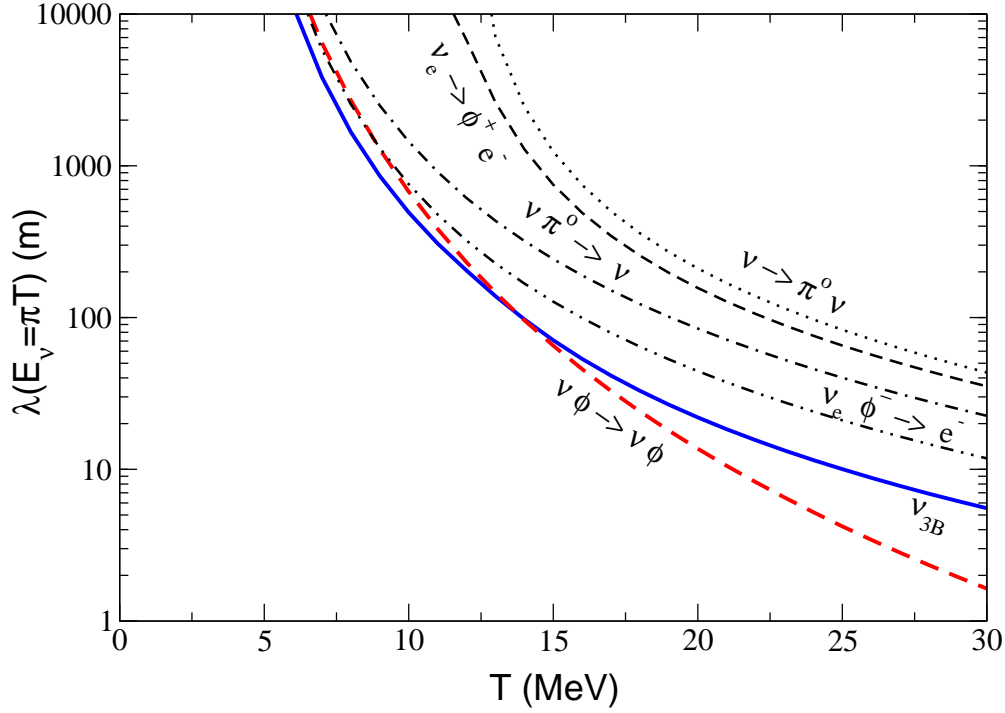


FIG. 3. Neutrino mean free path in a CFL meson plasma as a function of temperature. The neutrino energy $E_\nu = \pi T$ and is characteristic of a thermal neutrino.

neutral current scattering of neutrinos from charged pions and kaons is shown as the thick-dashed curve. As can be seen from the figure, this is the dominant source of opacity for $T \gtrsim 10$ MeV.

B. Neutrino Emissivity

The charged current decay of charged kaons and pions, and the novel decay of the neutral pion to a neutrino anti-neutrino pair are the leading one body process contributing to neutrino emission. In vacuum, the amplitude for similar processes are proportional the lepton mass due to angular momentum conservation. However, as discussed earlier the dispersion relations for Goldstone modes violate Lorentz invariance and consequently we find that the decay of finite momentum pions and kaons is not suppressed by the the electron mass (note that decay into muons is highly suppressed because the meson mass and the temperature are less than the mass of the muon). This can be understood by noting that the Goldstone

modes at finite density are collective excitations associated with deformations of the Fermi surface. In the rest frame of a meson that has finite momentum relative to the medium the Fermi Surface is not spherically symmetric. This breaks rotational invariance and angular momentum is no longer a good quantum number to describe the meson state. Consequently, the one body decay of the pions and kaons into massless lepton pairs is allowed.

The energy loss rate due to one body decays is computed using the standard formula

$$\epsilon_{1B} = \int \frac{d^3p}{(2\pi)^3 2E} \int \frac{d^3k_1}{(2\pi)^3 2E_1} E_1 \int \frac{d^3k_2}{(2\pi)^3 2E_2} |A|^2 (2\pi)^4 \delta^4(P - k_1 - k_2) \quad (13)$$

where P , k_1 and k_2 are the four momenta of the meson, the neutrino and the charged lepton respectively. We neglect the electron mass in the describing the kinematics of these reaction because the typical momenta of the particle are large compared to it. Further, since the electron chemical potential we find is also small compared to the temperature we are justified in neglecting the final state Pauli-blocking factor for the electrons. This allows us to perform the integration over the final state lepton momenta using the identity

$$\int \frac{d^3k_1}{2E_1} \int \frac{d^3k_2}{2E_2} \delta^4(P - k_1 - k_2) k_1^\mu k_2^\nu = \frac{\pi}{24} (P^\mu P^\nu + g^{\mu\nu} P^2) \quad (14)$$

to obtain the following result for the rate of energy loss from one body decays

$$\epsilon_{1B} = \frac{G_F^2 f_\pi^2 C^2}{6\pi} \int \frac{d^3p}{(2\pi)^3} f(E_p) ((\tilde{P} \cdot P)^2 - \tilde{P}^2 P^2). \quad (15)$$

where $P = (E_p, \vec{p})$ is the four momentum of the Goldstone boson and $C = \sin \theta_C$ for kaon decays, $C = \cos \theta_C$ for charged pion decays and $C = \sqrt{2}$ for the neutral current decay of the π^0 . The above processes can occur only when the meson four momentum is time like. Thus, only low momentum meson states (See Eq. (9)) can participate in the decay process. This accounts for the saturation of the one body decay contribution to the emissivity with increasing temperature seen in Fig. 4. The higher momentum, space like states can participate in processes such as $e^\pm \phi^\mp \rightarrow \nu$.

Processes involving two mesons in the initial state such as $\phi^\pm \phi^0 \rightarrow e^\pm \nu$ and $\phi^+ \phi^- \rightarrow \nu \bar{\nu}$ are likely to become important with increasing temperature. This is because the Goldstone

bosons are weakly interacting, the two particle amplitude is reduced by the factor p/f_π compared to the one body amplitude, where p is the relative momenta of the two Goldstone bosons. This might indicate that two particle processes will be relevant only for high temperatures of the order of f_π . However, surprisingly, we find that the two body rates become comparable to the one body rate for $T \sim 10$ MeV. This is because the meson dispersion relation becomes space like for momenta comparable to the meson mass. With increasing temperature the high momentum states get populated but are unable to decay via the one body process to lepton pairs because of kinematic restrictions. This is primary reason why we considered the two body processes ³. In Fig. 4, the rate of energy loss due to meson decay and two body reactions are shown. As discussed earlier, meson decay is the dominant reaction for $T \lesssim 10$ MeV. Reactions involving two particles in the initial state are also shown and become important at higher temperature. The purely leptonic process $e^+e^- \rightarrow \nu\bar{\nu}$ is also shown in the figure and is interestingly always smaller than the contribution arising from the mesons.

Other processes involving electrons in the initial state, such as $e^-\phi^+ \rightarrow \nu\phi^0$ could become important at low temperature where the electron density exceeds the meson density. We have ignored their contribution since this corresponds to $T \lesssim 5$ MeV where the one-body decay dominates. We also note when the temperature becomes comparable to the gap Δ neutrino emission reactions involving quark quasi-particles can become important. In particular, quark Cooper pair breaking has been shown to be relevant when $T \sim \Delta$ [20]. We expect the rate of this process to small at $T \sim 30$ MeV since it is suppressed by the factor $\exp(-2\Delta/T)$.

³It is interesting to note that in vacuum, with normal dispersion relations, the two body processes would dominate over one body decay at modest temperatures due to angular momentum restrictions on decay process.

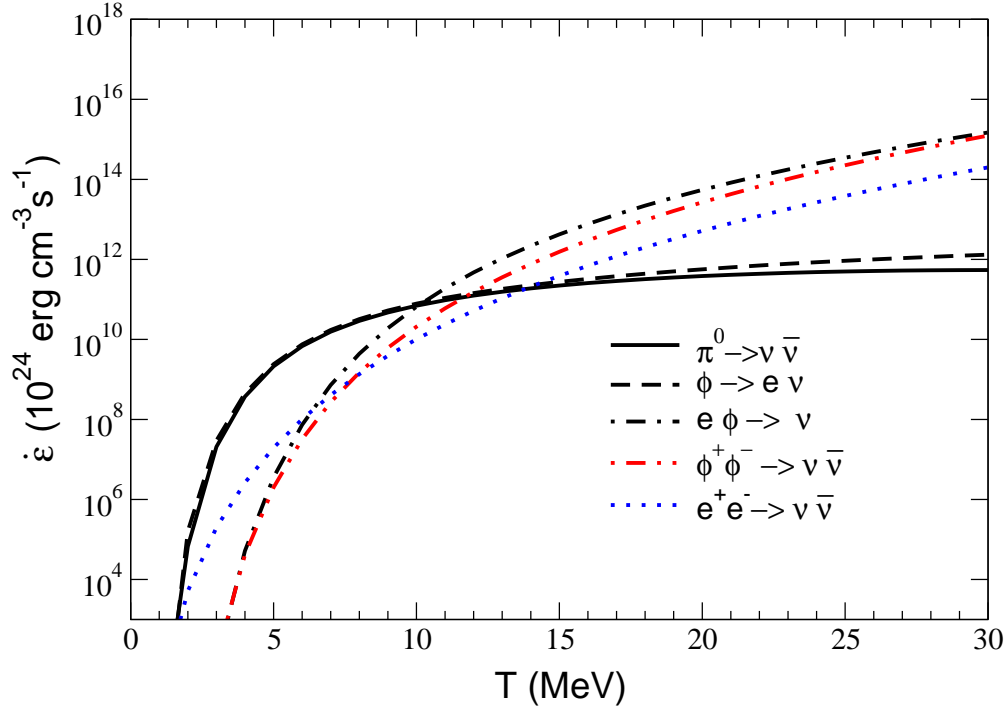


FIG. 4. Rate of energy loss due to neutrino emitting reactions. Contributions due to one body decay (solid curve), electron absorption on mesons (dot-dashed curve) and process involving the annihilation of two mesons is shown. The purely leptonic process $e^+e^- \rightarrow \nu\bar{\nu}$ is also shown (double dot-dashed curve).

IV. CONCLUSIONS

We have shown that novel processes in which mesons are either emitted or absorbed from energetic neutrinos occur in the CFL plasma and contribute to neutrino opacity. Even at zero temperature, high energy neutrinos, with energy large compared to the meson masses but still smaller than the gap scale have short mean free path as they can Cherenkov radiate mesons. At finite temperature, with the exponential growth of the meson number densities the mean free path rapidly decreases. Reactions such as $\nu + \pi^0 \rightarrow \nu$ and $\nu_e + \pi^- \rightarrow e^-$ are the dominant source of opacity at low temperature. We find that the mean free path for thermal neutrinos at $T = 10$ MeV is of the order of 100 meters while at $T = 5$ MeV the mean free path is larger than 10 kilometers –the typical size of the neutron star. For $T \gtrsim 10$

MeV, neutrino-meson scattering dominates the opacity and at $T = 30$ MeV we find the neutrino mean free path is only of the order of 1 meter. In the table below we compare the neutrino mean free path in CFL matter with those in nuclear matter and unpaired quark matter under similar conditions. To make these comparisons we employ earlier estimates of the neutrino mean free path in nuclear matter obtained by Reddy, Prakash and Lattimer [21] and in unpaired quark matter obtained by Iwamoto [22]. The quark chemical potential $\mu_q = 400$ MeV corresponds to a baryon density $n_B \sim 5n_0$ in quark matter, where $n_0 = 0.16 \text{ fm}^{-3}$ is the nuclear saturation density. We choose to compare the mean free path in these different phases at this density and the set neutrino energy $E_\nu = \pi T$.

phase	process	$\lambda(T=5 \text{ MeV})$	$\lambda(T=30 \text{ MeV})$
Nuclear Matter	$\nu n \rightarrow \nu n$	200 m	1 cm
	$\nu_e n \rightarrow e^- p$	2 m	4 cm
Unpaired Quarks	$\nu q \rightarrow \nu q$	350 m	1.6 m
	$\nu d \rightarrow e^- u$	120 m	4 m
CFL	$\nu \phi \rightarrow \nu \phi$	$> 10 \text{ km}$	1 m
	ν_{3B}	$> 10 \text{ km}$	6 m

The findings presented in the table above indicates that the neutrino mean free path in the CFL phase for $T \sim 30$ MeV is similar to that in unpaired quark matter. We find that the mean free path in the CFL phase remains comparable to that in unpaired quark matter down to $T \sim 15$ MeV. The mean free path in the CFL phase increase rapidly for $T \lesssim 10$ MeV as discussed earlier.

We have shown that novel neutrino emitting processes such as π^0 decay to neutrino-anti neutrino pairs occur in the CFL phase. Charged current leptonic decay of mesons is also enhanced in the medium. Both of the above occur because in the rest frame of the meson moving relative to the medium the ground state breaks rotational invariance. With increasing temperature, this enhancement saturates because only low momentum mesons have a time like dispersion relation. At higher temperatures, reactions involving two particles in the initial state overcome this kinematic constraint and dominate the emissivity. In the

neutron star context, the high temperature emissivity is unlikely to play an important role in neutron star dynamics because neutrinos are effectively trapped and are described by local thermal distributions. We will therefore restrict ourselves to $T \lesssim 10$ MeV to make the comparisons between the emissivity of the CFL phase with that of unpaired quark matter [22]. He finds the emissivity in unpaired quark matter due to beta decay of light quarks at $n_B = 5n_0$ to be $\dot{\epsilon}_{q\beta} \sim 2 \times 10^{36}$ erg cm⁻³ s⁻¹ at $T = 5$ MeV and $\dot{\epsilon}_{q\beta} \sim 2 \times 10^{38}$ erg cm⁻³ s⁻¹ at $T = 10$ MeV. This is to be compared with our finding that $\dot{\epsilon}_{CFL} \sim 5 \times 10^{33}$ erg cm⁻³ s⁻¹ at $T = 5$ MeV and $\dot{\epsilon}_{CFL} \sim 2 \times 10^{35}$ erg cm⁻³ s⁻¹ at $T = 10$ MeV. The emissivity is therefore roughly three orders of magnitude smaller. At lower temperature, the emissivity in the CFL phase is exponentially suppressed by the factor $\exp(-m/T)$, where m is the mass of the lightest meson due to the paucity of thermal mesons.

Our finding that the neutrino mean free path in the CFL phase are comparable to unpaired quark matter at $T \gtrsim 15$ MeV but vastly different at $T \lesssim 5$ MeV might impact the temporal aspects of neutrino diffusion in a newly born neutron star. It is also likely that the neutron star with a large CFL core will become transparent to neutrinos while still hot with $T \sim 5 - 10$ MeV. This might affect the late time supernova neutrino emission. In particular, we expect it to increase both the luminosity and the average energy of the emitted neutrinos. In order to gauge how the physics of high density neutron star core will impact observable aspects of early neutron star evolution the rates computed in this work need to be included in detailed numerical simulations of core collapse supernova. This is the only reliable means to bridge the gap between the exciting theoretical expectation of color superconductivity at high density and the observable aspects of core collapse supernova – the neutrino count rate, the neutrino spectrum and the explosion itself.

Acknowledgements

We thank David Kaplan, Krishna Rajagopal and Misha Stephanov for useful comments. This work is supported in part by funds provided by the U.S. Department of Energy (D.O.E.) under cooperative research agreement DF-FC02-94ER40818. M. S. was supported in part by the Polish State Committee for Scientific Research, (KBN) grant no. 2P 03B 094 19. M. T. was supported in part by Grant-in-Aid for Scientific Research from Ministry of Education, Science, Sports and Culture of Japan (No. 3666).

REFERENCES

- [1] M. Alford, K. Rajagopal and F. Wilczek, Nucl. Phys. B **537**, 443 (1999) [hep-ph/9804403].
- [2] M. G. Alford, K. Rajagopal and F. Wilczek, Phys. Lett. B **422**, 247 (1998) [arXiv:hep-ph/9711395].
- [3] R. Rapp, T. Schafer, E. V. Shuryak and M. Velkovsky, Phys. Rev. Lett. **81**, 53 (1998) [arXiv:hep-ph/9711396].
- [4] K. Rajagopal and F. Wilczek, arXiv:hep-ph/0011333.
- [5] M. G. Alford, K. Rajagopal, S. Reddy and F. Wilczek, Phys. Rev. D **64**, 074017 (2001) [arXiv:hep-ph/0105009].
- [6] M. G. Alford, J. Berges and K. Rajagopal, Nucl. Phys. B **571**, 269 (2000) [arXiv:hep-ph/9910254].
- [7] D. Blaschke, T. Klahn and D. N. Voskresensky, Astrophys. J. **533**, 406 (2000) [arXiv:astro-ph/9908334].
- [8] D. Page, M. Prakash, J. M. Lattimer and A. Steiner, Phys. Rev. Lett. **85**, 2048 (2000) [arXiv:hep-ph/0005094].
- [9] G. W. Carter and S. Reddy, Phys. Rev. D **62**, 103002 (2000) [arXiv:hep-ph/0005228].
- [10] A. Burrows and J. M. Lattimer, Astrophys. J. **307**, 178 (1986). W. Keil and H. T. Janka, Astron. Astrophys. **296**, 145 (1995). J. A. Pons, S. Reddy, M. Prakash, J. M. Lattimer and J. A. Miralles, Astrophys. J. **513**, 780 (1999) [astro-ph/9807040].
- [11] R. Casalbuoni and R. Gatto, Phys. Lett. B **464**, 111 (1999) [arXiv:hep-ph/9908227].
- [12] D. T. Son and M. A. Stephanov, Phys. Rev. D **61**, 074012 (2000) [hep-ph/9910491]; erratum, *ibid.* D **62**, 059902 (2000) [hep-ph/0004095].

- [13] C. Manuel and M. H. Tytgat, Phys. Lett. B **479**, 190 (2000) [arXiv:hep-ph/0001095].
- [14] S. R. Beane, P. F. Bedaque and M. J. Savage, Phys. Lett. B **483**, 131 (2000) [arXiv:hep-ph/0002209].
- [15] T. Schafer, arXiv:hep-ph/0109052.
- [16] P. F. Bedaque and T. Schafer, hep-ph/0105150.
- [17] D. B. Kaplan and S. Reddy, arXiv:hep-ph/0107265.
- [18] T. Schafer, arXiv:hep-ph/0201189.
- [19] R. Casalbuoni, Z. Duan and F. Sannino, Phys. Rev. D **63**, 114026 (2001) [arXiv:hep-ph/0011394].
- [20] P. Jaikumar and M. Prakash, Phys. Lett. B **516**, 345 (2001) [arXiv:astro-ph/0105225].
- [21] S. Reddy, M. Prakash and J. M. Lattimer, Phys. Rev. D **58**, 013009 (1998) [arXiv:astro-ph/9710115].
- [22] N. Iwamoto, Ann. Phys. **141**, 1 (1982)